Advancing Accuracy of Shooting and Bouncing Rays Method for Ray-Tracing Propagation Modeling Based on Novel Approaches to Ray Cone Angle Calculation

Stephen Kasdorf, *Student Member, IEEE*, Blake Troksa, *Student Member, IEEE*, Cam Key, *Student Member, IEEE*, Jake Harmon, *Student Member, IEEE*, and Branislav M. Notaroš, *Fellow, IEEE*

***Abstract*—We propose and evaluate several improvements to the accuracy of the shooting and bouncing rays (SBR) method for ray-tracing (RT) electromagnetic modeling. We propose per-ray cone angle calculation, with the maximum separation angle between rays calculated for every individual ray, based on a set of local neighbors rather than a single global maximum. This allows the smallest theoretical error of the SBR method, adaptive ray spawning procedures, and a unique analysis of the effect of ray cone sizes on the accuracy of the method. For the conventional uniform angular distribution of rays, a less general and versatile but more expeditious approach, we derive an analytical expression for the optimal choice of cone angle to again maximize the overall accuracy of the SBR computation. Both approaches are derived using icosahedral ray spawning geometry and adjacent ray sets, which are also used for our double counted rays identification and removal technique that avoids complicated ray path searches. The results demonstrate that the advanced shooting and bouncing RT method—using both proposed ray cone generation approaches—can perform wireless propagation modeling of tunnel environments with the same accuracy as image theory RT, a dramatically less efficient but traditionally considerably more accurate solver.**

***Index Terms* – Wireless propagation modeling, asymptotic high-frequency techniques, propagation in large tunnels, ray tracing method, shooting bouncing rays techniques, ray cone angles, double count removal, image theory ray tracing.**

I. Introduction

As communications frequencies become higher and the propagation environments that need to be electromagnetically characterized become physically larger and more interconnected given the increased complexities and demands of emerging wireless system functionalities, these structures become more difficult to model using full-wave computational electromagnetics (CEM) techniques. For example, CEM modeling and simulation of wireless signal propagation in tunnels of underground mines or traffic (e.g., railway or subway) systems presents extraordinary challenges and is an open CEM research problem with unparalleled difficulty in many of its aspects. A mine or traffic tunnel at wireless communication frequencies is electrically an extremely large electromagnetic system, typically spanning thousands of wavelengths. High-frequency asymptotic techniques have been shown to be computationally efficient at modeling such structures [1]–[4].

Indeed, there has been a "renaissance" of CEM simulations and computations using high-frequency, asymptotic methodologies and implementations and renewed and growing interest in their applications to wireless propagation modeling within indoor and outdoor communication environments. While asymptotic methods for numerically approximate high-frequency modeling can never be as accurate as the full-wave methods for numerically rigorous field computation, it appears that there are opportunities for the improvement of accuracy of asymptotic modeling in some of its components and aspects. This paper addresses the accuracy of ray-based high-frequency modeling in general and when particularly applied to wireless propagation modeling of tunnel environments.

One of the most important classes of asymptotic techniques for CEM modeling is constituted by the ray tracing (RT) approach, based on the theory of geometrical optics (GO), by which the electric field is discretized into rays, with two common methods used for RT simulations, (i) the image theory method (IT) and (ii) the shooting and bouncing rays (SBR) method. The IT approach uses the method of image transformation to mirror a transmitter across reflection planes in the environment to find exact propagation paths from the transmitter to a receiver. From the accuracy standpoint, this method is advantageous due to the exact paths computed, making the phase error negligible. The only sources of phase error stem from geometric mesh approximations and numerical truncation, the latter typically being insubstantial compared to the former. However, the computational complexity of the IT method is $O(N^K)$ where N is the number of planar facets in the model and K is the number of

Manuscript received January 9, 2020, revised October 26, 2020. This work was supported by the National Science Foundation under grant ECCS-1646562.

Stephen Kasdorf, Blake Troksa, Cam Key, Jake Harmon, and Branislav M. Notaroš are with the Department of Electrical and Computer Engineering, Colorado State University, Fort Collins, CO 80523-1373 USA (e-mail: skasdorf@rams.colostate.edu, blake.troksa@gmail.com, camkey@rams.colostate.edu, j.harmon@colostate.edu, notaros@colostate.edu).

reflections [5]. In electrically extremely large, closed environments, many rays and reflections are needed for adequate sampling, making IT impractical despite its attractive accuracy characteristics.

The SBR method, in contrast, launches rays from a transmitter in every direction, each ray is tracked as it propagates through the geometric environment according to Snell's law, and its magnitude is adjusted according to Fresnel's coefficients [1]. These paths are then tested to determine if the ray intersects a receiver, in which case its electric field is added to the field at the receiver point. The ray paths are inexact, so further phase error is introduced in the SBR method compared to the IT method. However, the computational complexity of SBR, $O(NK)$, where N is the number of rays spawned and K is the number of reflections, is substantially lower than that of IT. Additionally, the SBR method allows for the extension of propagation to include refraction and diffraction, which IT alone cannot accomplish. This makes the SBR method much more efficient and versatile for use in large environments.

Previous work has demonstrated the effectiveness of the SBR method in tunnel environments, with findings showing that this method is a useful simulation technique for large, complex environments. The accuracy of the approach, however, is poor when compared to IT and full-wave techniques [3]. In [5], the SBR model was shown to be ineffective at simulating fields in tunnel environments further than a few hundred meters. This is due to issues with ray receptions in the SBR model. The so-called SBR cones method uses reception spheres to model the reception of a wavefront at a receiving antenna, where the sizes of these spheres are extremely important for the accuracy of the SBR method [3]. With large spheres, the results become inaccurate due to multiple counting of propagating wavefronts. Too small of a sphere size, on the other hand, causes discontinuities in the wavefront, known as undercounting. Previous work has been done in determining the appropriate sizes of the reception spheres by using spheres of variable size determined by path length [3],[4],[6]–[10]. However, these works assume that the ray distribution is uniform across the three-dimensional (3-D) spawning volume, and this assumption is invalid in 3-D, which can lead to inaccuracies.

This paper presents the development of an SBR model and analysis and improvement of the accuracy of the SBR computation based on three factors and associated novel contributions. Specifically, we theoretically and empirically analyze importance of the distribution angle of rays launched from the transmitter for phase accuracy, coupled with the importance of ray double count removal for magnitude accuracy. Firstly, we propose per-ray cone angle calculation, with the maximum separation angle calculated for every individual ray based on a set of local neighbors rather than a single global maximum. This allows the smallest theoretical error of the SBR method, with undercounting being completely removed from the model, as well as decreasing the ray cone size which substantially reduces the phase error. Secondly, we also analyze constant angular distributions of the rays, which allow for much more expeditious simulations but make the overall accuracy of the computation extremely sensitive to the choice of the angular distribution. Here, we derive an analytical expression for the optimal choice of this angle to maximize the overall accuracy of the SBR computation, and demonstrate empirically that the SBR simulations generated using the derived optimal constant angle are indistinguishable from those generated using per-ray angles, that is, from the theoretical best-case scenario for simulation accuracy. Thirdly, the two approaches to ray cone angle calculation are coupled with a double counted rays identification and removal approach using icosahedron geometry and neighbor ray sets to identify and remove double counted contribution without the need for lengthy and complicated path searches based on the full geometry of the ray paths, hence coupling improvements of phase and magnitude accuracies. We thus demonstrate how the SBR methodology and implementation can be advanced to produce an SBR approach of similar accuracy as the image theory RT method, in simulations of large tunnels. The results show that, with the proposed, implemented, and analyzed accuracy improvements, the SBR method can perform wireless propagation modeling of planar tunnel environments with the same accuracy as the dramatically less efficient image theory approach. The three contributions to the SBR methodology are completely general, and thus are capable of being applied to any existing SBR method, model, and simulation. These advancements are positioned and capable of increasing accuracy of an existing SBR technique to a point where the results are almost indistinguishable from the IT approach, as demonstrated in this paper. In fact, this demonstration is the fourth novel contribution of this work, as it has always been thought that the accuracy of the SBR approach can never be brought to the level of the IT accuracy. Note that the basic theory and preliminary accuracy validation of our SBR RT analysis of tunnels are presented in a summary form in [11].

II. SBR Methodology

A. Ray Receptions

Once rays have been tracked as they propagate through a medium, they are tested to see if there is an intersection of the ray and a receiving antenna. The cones technique is advantageous here, because the regular, circular cross-section of the ray bundle. Reception points for the rays are modeled as growing spheres which represent the growing cross-section of the ray cone. An intersection test between the sphere and the center ray of the cone is used, as shown graphically in Fig. 1, which is computationally simple and efficient. If this center ray intersects a receiver sphere, one of the rays represented in the ray cone is an exact hit. The linear nature of Maxwell's equations results in the field at any receiver point being the linear superposition of all electric field contributions of rays that intersect this point.

The radius of the ray cones, and thus the reception spheres, is determined for the ith ray by

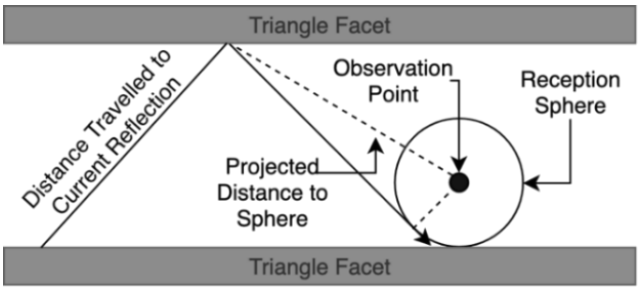

Fig 1. Ray–sphere intersection: graphical representation for the scene of a ray approaching a sphere and the corresponding components used in the calculation of the reception sphere radius.

$$r_{sphere_i} = \frac{\alpha_i d_i}{\sqrt{3}} \tag{1}$$

where d_i is the total distance a ray has travelled and α_i is the maximum separation angle between a ray and its neighbors [3]–[10]. This equation calculates the minimum possible ray cone radius that fully covers the electric field radiation. In tunnel environments, it is possible to have multiple reflected wavefronts received from the source. However, the propagation distance is tracked individually with every ray, so this can be applied independently for each ray.

B. Double Count Removal Method

The SBR approach requires launching discrete rays, each of which representing a cone of influence to fully cover the transmitting radiation pattern. Any places where the cones do not overlap would represent a non-physical scenario, where receptions might be missed in the simulation, constituting undercounting. To fully cover the 3-D radiation pattern without discontinuities in the field, the cones must overlap, as shown in Fig. 2. This overlap represents a substantial drawback as the overlapping wavefronts can be represented at least twice in the simulation. Any intersection of the overlapping wavefronts with a receiver will lead to the electric field from a single wavefront contributing twice to the total field, which is referred to as double counting [7],[8],[10]. The double counted fields can be removed but require searching ray paths to find common images. This shows the important role both the ray distribution and cone sizes play in the accurate implementation of the SBR method.

The spawning techniques for the ray tracing application involve sampling points on surfaces that surround some ray origin point. Once these sampled points are determined, each ray for the ray tracing algorithm is launched from the origin to one of the sampled points. While different spawning techniques such as uniform grid sampling and Fibonacci spiral sampling have been tested and provide various advantages regarding sample spacing and ease of formation [1],[2],[12], we use here an icosahedron for the sampling method. Each face of an icosahedron is subdivided into equilateral triangles, where the number of vertices is given according to the nth triangular number. The rays are launched on the vertices of the subdivided icosahedron face with the number of rays launched on a face being $n(n+1)/2$, where n is the number of subdivisions along an edge of the face. This allows for very uniform distribution of launched rays, which is a requirement for accurate SBR simulations. Additionally, the icosahedron provides important topological information about the rays; the rays can be grouped together into sets of neighbor rays. These neighbor rays can be used to calculate the angle between rays, which proves extremely useful in calculating the sizes of ray cones, as will be discussed in detail in Section III. Similar methods of ray spawning, such as normalized cube which subdivides cubes instead of triangles, offer similar ray topology benefits. The ray neighbor sets can also be used to remove double counted rays in a novel way. Namely, the double counts can only occur with overlapping ray cones, where the overlap represents the same wavefront. Any two ray cones that overlap and take the same path from the source to the receiver must represent the same wavefront which therefore will be counted twice. So any two rays that are neighbors that take the same number of reflections from the source to the receiver will be double counted, and one is easily removed.

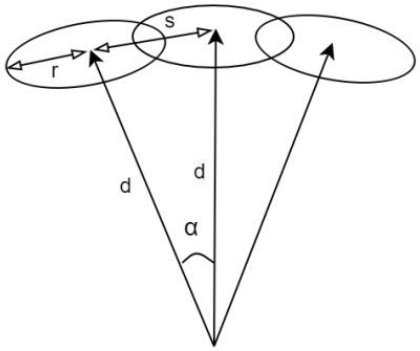

Fig. 2. Geometry of showing an adjacent and non-adjacent ray cone.

To prove that overlap, and thus double counted wavefronts, is limited to adjacent ray sets, we can use the geometry shown in Fig. 2. The condition that must be satisfied is $s/2 < r < s$. This condition ensures overlap between adjacent rays to provide full radiation coverage, while preventing overlap between non-adjacent rays. From the figure, and using the law of cosines, we get $s = \sqrt{2d^2(1-\cos\alpha)}$. Assuming that α is small and taking the small angle approximation of $\cos\alpha$, we get that $s \approx \alpha d$. Thus, the inequality becomes,

$$\frac{\alpha d}{2} < r < \alpha d. \tag{2}$$

As long as α is chosen as the largest angle between a ray and its neighbors, then the left-hand side of the inequality ensures full radiation pattern coverage. We see that (1) satisfies (2), showing that it is a good choice for the radius of the ray cone. Equation (2) leads to two important conclusions: (i) Because ray cone overlap is limited to adjacent rays, the path search can be limited to only a neighbor ray set, which drastically reduces the computational complexity of double count removal; (ii) This highlights the importance of choosing α correctly. If this angle is taken to be a constant value for instance, it is possible to cause undercounting since ray distribution is not constant and it is possible that not all ray

cones overlap with all adjacent rays. Undercounting is problematic because it cannot be identified in post-processing. Choosing a constant value that is too large can also lead to cone overlap between non-adjacent rays, which expands the search for double count removal.

For the context, previous work in double count removal uses one of two common methods, where in the first approach, a characteristic sequence of a ray's path can be tracked, and any rays at the same receiver with the same characteristic sequence represent a double count, such as in [10]. However, this method quickly exhausts available memory, in addition to lacking parallelizability. The second method uses geometric path searches to identify double counted rays by calculating the distance between rays at a reception and removing those that are within the cone radius, such as in [7],[8]. However, this technique requires a large number of memory accesses and thus represents a bottleneck in the simulation. Our double count removal technique requires no additional memory storage because the adjacent ray sets are calculated only once in the preprocessing portion of the simulation. Additionally, memory checks are limited due to only having to search a single set instead of multiple ray distance accesses. This means that our method not only is computationally more efficient, but it is also more memory friendly, which allows for larger and faster simulations.

III. Per-Ray and Optimal Constant Ray Cone Angle Calculations

There is a very important relationship between ray cone sizes and simulation accuracy. In the SBR model, the distribution of rays being launched from a receiver becomes vital for the accuracy of the model, where an even distribution is desired [6]. However, when launching rays in 3-D, it is not possible to have exactly uniform distribution of rays.

We choose the inscribed icosahedron spawning pattern because of its regular and predictable angular distribution of rays. Equation (1) gives the radius of the ray cones required for full radiation pattern coverage with the minimum possible overlapping of the cones. This formula requires that the angle α is the maximum angle between neighbor rays. Generally, the distribution of ray angles is assumed to be approximately uniform, and a constant value of α is used to calculate ray cone sizes. On the other hand, as can be seen in Fig. 3, the angular distribution of rays is significantly larger at the centers of the icosahedron faces and is smallest at the vertices. For other ray spawning patterns, this discrepancy is typically even more pronounced. This variation in angular distribution between rays can prove to be problematic if a constant α is assumed (unless the proper value for α is chosen).

Using the adjacent ray sets developed for use in double counted ray identification, we can also calculate the maximum angle between rays for every individual ray. This is advantageous for several reasons. Firstly, using these individual α values allows for the smallest theoretical error of this SBR method, because cone sizes are as small as possible for every ray while ensuring full radiation coverage, which

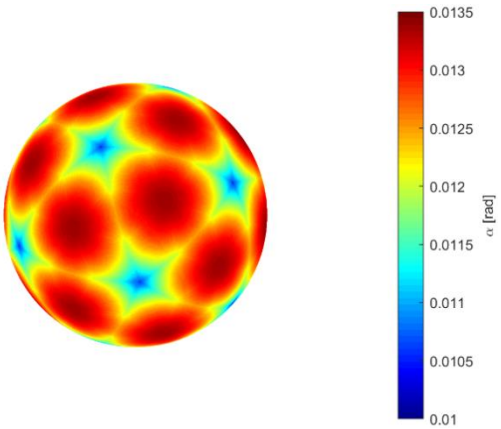

Fig. 3. Angular distribution of rays on an icosahedron: distribution of the maximum angle between neighbor rays (α) across an icosahedron spawning procedure with $n = 100$ subdivisions along an edge of the icosahedron face.

minimizes phase error. In complicated environments where cone cutoff is an issue, this method of calculating cone size will allow for the smallest possible error. Additionally, in adaptive ray spawning procedures, the method of calculating angular distributions for every ray allows for arbitrary refinement of the ray spawning while keeping physical interpretation of ray tube sizes. Lastly, per-ray calculations of angular distributions of rays allows for a unique analysis of the effect of ray cone sizes on the accuracy of the method.

If a constant angular distribution is assumed, this value must be chosen wisely so that error in the method is minimized. If α is chosen to be too small, the cones calculated on rays at the center of an icosahedron face will be too small, leading to a lapse in radiation pattern coverage, namely, undercounting. These field lapses grow as rays propagate in large structures, leading to large errors in the simulation. Fig. 4(a) shows a face of the icosahedron with cones inscribed calculated with too small an angle.

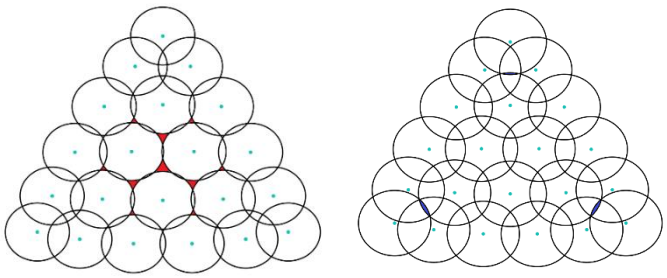

Fig. 4. Illustration of ray cones calculated based on (1) with $d = 1$ and (a) α chosen smaller than the optimal value, with lapses in radiation coverage being filled in red, and (b) α chosen larger than the optimal value, with overlaps between non-adjacent ray cones being filled in blue.

On the other hand, if α is chosen to be larger than the optimal value, then cones will become too large towards the vertices of the icosahedron. This means that the cutoff issue will be more significant in these cases. Furthermore, non-adjacent ray cones will start to overlap, leading to triple or quadruple counting of field contributions. These overlaps will not be identified in the double count identification procedures, meaning that this can lead to error in the model. A case with

the cones calculated using α greater than ideal is shown in Fig. 4(b).

Based on Figs. 3 and 4, the most sensible choice of α for cones with the minimum overlap is the greatest maximum ray angle across the whole face. This ray lies in the center of the icosahedron face as seen in Fig 3. The optimal angle can be found analytically using the golden ratio, with the radius of a sphere inscribed in a regular icosahedron being [13]

$$r = \frac{\phi^2}{2\sqrt{3}}a = \frac{\sqrt{42+18\sqrt{5}}}{12}a \approx 0.755a \tag{3}$$

where ϕ denotes the golden ratio and a is the edge length of the icosahedron. The edges are subdivided equally in a regular icosahedron so that the segment length is the edge length divided by the number of segments, $l = a/(n-1)$, with n again standing for the nth triangular number used in icosahedron subdivision. This scenario is shown graphically in Fig. 5, from which it is apparent that $\alpha = \tan^{-1}(l/r)$. After some rearranging, we are left with

$$\alpha = \tan^{-1}\frac{2\sqrt{3}}{\phi^2(n-1)} = \tan^{-1}\frac{12}{(n-1)\sqrt{3}(3+\sqrt{5})} \tag{4}$$

This equation for optimized α is verified and tested in Section IV.

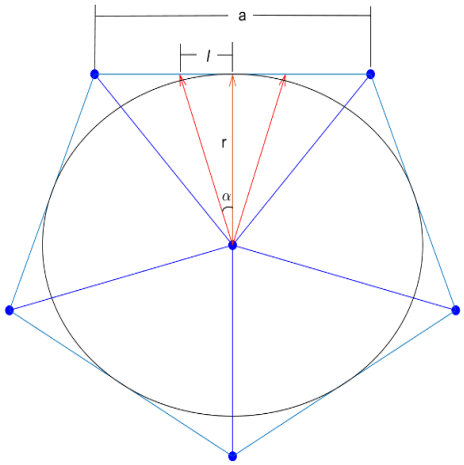

Fig. 5. Circle inscribed in an icosahedron: the radius of the inscribed sphere is given in terms of the edge length of an icosahedron face via the golden ratio.

IV. Results and Discussion

Validation of the advanced SBR RT technique and demonstration of the accuracy improvements are presented here using several tunnels of different uniform cross sections. Tunnels are chosen as a challenging environment for RT solvers, due to the large distances covered and the higher order modes present in propagation. Tunnels offer a corner case enabling a rigorous test for SBR algorithms. The simulations in these tests were performed by creating a line of reception points directed down the long axis (z-axis) of the tunnels at evenly separated intervals. The solutions obtained using the presented SBR RT algorithm are compared with computed results of other asymptotic and full-wave CEM solvers that offer state-of-the-art performance for tunnel simulation.

A. Validation Against Image Theory

The first set of results is for comparison against an IT simulation. While IT is still an asymptotic approximation, it represents the perfect case for ray-based methods since the phase error is almost entirely eliminated. Our SBR method is compared to IT in a rectangular dielectric waveguide with cross-sectional dimensions 4 m × 4 m × 1000 m [3]. The rectangular waveguide is particularly appropriate for comparison with SBR because of the accuracy of IT in this structure. In planar geometries, IT produces the most accurate ray tracing results [3]. The waveguide is excited with a vertically polarized isotropic transmitter at 1 GHz located at (x, y, z) = (1.1 m, 2.1 m, 0), with the x, y, and z coordinates being measured from the bottom left corner of the opening of the waveguide when viewed toward the wave propagation. The receivers are also isotropic and located at (1.9 m, 1.7 m, z), chosen to avoid any advantage due to symmetries in the simulation. The tunnel wall parameters are relative permittivity $\varepsilon_r = 5$ and conductivity $\sigma = 0$.

In Fig. 6, we see that the SBR solution agrees very well with the IT reference results. The SBR method uses α calculated per ray, showing that this technique is viable for simulating very large-scale environments. In fact, we observe a perfect match of the two sets of results as far as 1,000 m down the tunnel, which is a truly exceptional result that demonstrates an ability of our SBR RT method to correctly compute transmission path lengths at very large distances from the transmitter, a feature traditionally reserved for the dramatically less efficient image-theory RT.

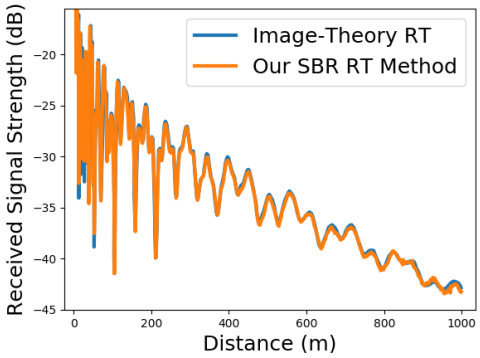

Fig. 6. Comparison of the presented SBR method with IT [3] in a dielectric ($\varepsilon_r = 5$, $\sigma = 0$) waveguide at 1 GHz [transmitter at (1.1 m, 2.1 m, 0), receivers at (1.9 m, 1.7 m, z)].

B. Double Count Removal

Since the SBR results in Fig. 6 match so well with IT, this case also seems ideal for examination of the effects of double counting on the accuracy of the model. Fig. 7 shows the absolute errors of SBR results with respect to reference IT data computed with and without double count removal, respectively. The results emphasize the substantial impact that the double counted rays have on the accuracy of SBR simulations. When compared to results in [7] and [10], we observe a similar error reduction from our technique as those

in existing literature. This shows that the proposed technique similarly reduces the computation error while drastically reducing the complexity of the double count removal search.

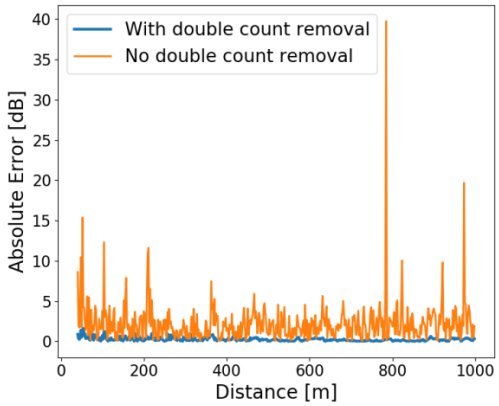

Fig. 7. Double count removal results. Absolute error in dB of our SBR simulation with respect to the reference IT results [3] for the dielectric waveguide with and without double count removal.

C. Ray Cone Angles

Next, we compare the model's ability to use a constant angular distribution given in (4). The per-ray α calculations are the theoretical best-case scenario for simulation accuracy, so simulations using constant α are compared to the per-ray α case. We generate simulations with an assumed constant α and plot mean absolute error of the simulation when compared to IT results. In this way, we expect that the mean absolute error is at a minimum when using the analytical expression derived in (4). The results of this comparison are shown in Fig 8. We draw several interesting conclusions upon examining these results. Firstly, the value of α predicted by (4) perfectly matches with the lowest error in every case. This empirically demonstrates that the derived value of α is indeed optimal. Additionally, we see that the error also increases after this optimal α as expected. The increase in error after the optimal value is smaller than expected. The reason for this comes in two parts. First, with such a regular structure as the rectangular dielectric waveguide, the tube cutoff that is expected with cones that are too large does not happen, so this does not contribute to the error in this case. In an analysis on a more complex and nonuniform structure, we expect the error to jump up more drastically. Second, we expected an increase in error due to ray cone overlap on non-adjacent rays. In these tests, the face of the icosahedron is oriented down the length of the waveguide, which means that the rays with extra overlap do not penetrate far into the length of the structure. This means that the error will not jump up drastically in this case either.

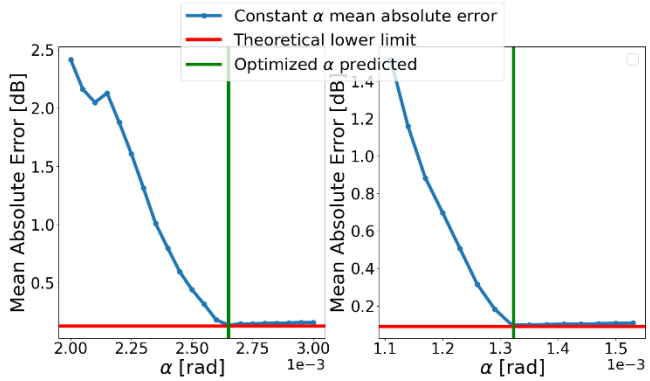

Fig. 8. Mean absolute error of SBR calculation using a constant angular distribution, with respect to reference IT results, with the vertical line marking the optimal value of α predicted with (4) and the horizontal line representing the error using per-ray α: results for (a) N = 500 subdivisions and (b) N = 1001 subdivisions.

D. Comparison to Full-Wave Simulation

Next, we compare the SBR simulation to a full-wave technique for a mine tunnel with an arched ceiling presented in [14], where the tunnel is modeled using the surface integral equation (SIE) technique accelerated by the fast multipole method in conjunction with the fast Fourier transform (FMM-FFT). The FMM-FFT accelerated SIE simulations of mine environments are rigorously verified by comparison against measurements [14]. The tunnel considered here has an irregular, curved cross section. However, the SBR methodology encounters difficulty when planar segments are used to approximate curvature, because many segments can lead to many non-physical images produced in the model. Due to these issues, the curvature is approximated using an equivalent rectangular cross-section approach, as shown in [15]. The results of the SBR and FMM-FFT-SIE simulations, with the material parameters of tunnel walls being $\varepsilon_r = 5.5$ and $\sigma = 0.15$ S/m and the operating frequency 915 MHz, are displayed in Fig. 9.

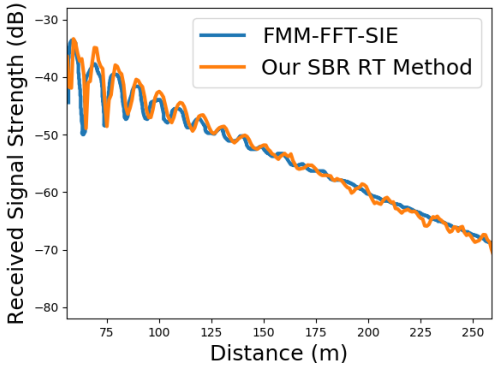

Fig. 9. Comparison of the SBR ray-tracing solution to the FMM-FFT accelerated SIE simulation of a mine tunnel with arched ceiling [14]. The tunnel is excited with a 915-MHz vertically polarized Hertzian dipole antenna and the material parameters are $\varepsilon_r = 5.5$ and $\sigma = 0.15$ S/m.

We see an excellent agreement between our SBR method and the full-wave technique. This SBR simulation is generated using α derived in (4), but the results generated using per-ray angles are indistinguishable from the results in Fig. 9. This shows the robust nature of the proposed SBR technique and its ability to provide accurate modeling of wireless propagation in large environments. Moreover, while providing comparable accuracy in the tunnel simulation, the proposed SBR RT technique is dramatically more efficient than the fast full-wave solver; the FMM-FFT-SIE solver takes

over 19 hours to simulate this environment on a multi-GPU cluster [14], compared to less than 1 minute for the SBR technique on a modest single-GPU desktop.

V. Conclusion

This paper has proposed and presented the shooting and bouncing rays method for ray-tracing modeling with improved accuracy, with accuracy improvements coming from several components of the SBR computation. The paper has examined the effect of the calculated sizes of the SBR ray cones on the accuracy of the simulations, proving a very high importance of the proper choice of the distribution angle for the overall performance of the SBR method. We have proposed calculating the ray cone sizes based on the maximum separation angle for every ray, individually. This per-ray calculation is an excellent choice in very complex environments and allows for adaptive ray spawning techniques to be implemented, but it comes at the cost of increased computational complexity in the model. The alternative is to assume a constant angular distribution of the rays, which allows for much more expeditious simulations but makes the overall accuracy of the computation extremely sensitive to the choice of the angular distribution. The paper has given the optimal choice for this angle, which has been shown to be viable in large tunnel environments. Additionally, we have shown the importance of removing double counted phase fronts in the SBR method that implements the ray cones approach. The presented technique uses icosahedron geometry and adjacent ray sets to identify and remove double counted ray contribution without the need for the analysis of the full geometry of the ray paths and lengthy path searches. The improvement of the magnitude accuracy due to the double count removal couples with the improvement of the phase accuracy associated with the optimal distribution angle of rays launched from the transmitter.

The results have demonstrated that the SBR method with the proposed, implemented, and evaluated accuracy improvements can perform wireless propagation modeling of tunnel environments with the same accuracy as the image theory RT, a computationally much slower but traditionally more accurate solver. We have shown a perfect match of the improved SBR method and the IT method for a kilometer-long tunnel, where it is important to note that correct computation of transmission path lengths at very large distances from the transmitter is a feature traditionally reserved for the dramatically less efficient image-theory RT. We have shown the SBR model's ability to effectively use both the per-ray α calculations and an analytically derived constant angular distribution. The results have empirically demonstrated that the derived value of α is indeed optimal. The SBR simulations generated using the derived optimal constant α are indistinguishable from those generated using per-ray angles, the latter α calculations being the theoretical best-case scenario for simulation accuracy. This demonstrates the robustness and usability of both approaches. The example with comparison of the advanced SBR method with the FMM-FFT accelerated SIE simulations has demonstrated the accuracy of the proposed SBR RT technique in analysis of electromagnetic wave propagation in mine tunnel environments comparable to a full-wave solution, while benefiting from the efficiency of computation characteristic for asymptotic ray-based methods.

Overall, the main contribution of this work is an SBR ray-tracing method of similar accuracy as the IT RT approach. While demonstrated for electromagnetic propagation modeling of large tunnels, the proposed accuracy improvements of this SBR methodology should prove beneficial in other applications, either on its own or hybridized with other CEM approaches, in indoor and outdoor wireless propagation modeling. With growing challenges imposed by emerging communication technologies, e.g., *n*G communication systems, the "renaissance" of asymptotic CEM simulations will just be intensified, and hence a need for this and similar advancements of SBR and other general classes of asymptotic CEM techniques.

References

[1] H. Ling, R.-C. Chou, and S.-W. Lee, "Shooting and bouncing rays: calculating the RCS of an arbitrarily shaped cavity," in *IEEE Transactions on Antennas and Propagation*, vol. 37, no. 2, pp. 194-205, Feb. 1989.

[2] B. Troksa, C. Key, F. Kunkel, S. V. Savic, M. M. Ilic, and B. M. Notaros, "Ray Tracing Using Shooting-Bouncing Technique to Model Mine Tunnels: Theory and Verification for a PEC Waveguide," invited paper, Special Issue on Advanced Computational Electromagnetic Methodologies and Techniques, *ACES Journal*, Vol. 34, No. 2, February 2019, pp. 224–225.

[3] D. Didascalou, "Ray Optical Wave Propagation Modelling in Arbitrarily Shaped Tunnels," Ph.D. dissertation, Dept. Elect. Eng., *Universität Karlsruhe*, Karlsruhe, Germany, 2000.

[4] S.-H. Chen and S.-K. Jeng, "SBR image approach for radio wave propagation in tunnels with and without traffic," *IEEE Transactions on Vehicular Technology*, vol. 45, no. 3, Aug. 1996, pp. 570-578.

[5] N. Sood, "Realistic Assessment of Novel Wireless Systems with Ray-Tracing Based Techniques," MASc Thesis, Dept. Elect. Comp. Eng., *Univ. of Toronto*, Toronto, Canada, 2012.

[6] M. F. Cátedra and J. Perez, Cell Planning for Wireless Communications. Norwood, MA, USA: Artech House, 1999.

[7] N. Noori, A. A. Shishegar and E. Jedari, "A New Double Counting Cancellation Technique for Three-Dimensional Ray Launching Method," *2006 IEEE Antennas and Propagation Society International Symposium*, Albuquerque, NM, 2006, pp. 2185-2188.

[8] V. Mohtashami and A. A. Shishegar, "A new double—counting cancellation technique for ray tracing using separation angle distribution," *2008 IEEE International RF and Microwave Conference*, Kuala Lumpur, 2008, pp. 306-310.

[9] Z. Yun and M. F. Iskander, "Ray Tracing for Radio Propagation Modeling: Principles and Applications," *IEEE Access*, vol. 3, pp. 1089-1100, 2015.

[10] Z. Yun, M. F. Iskander and Z. Zhang, "Development of a new shooting-and-bouncing ray (SBR) tracing method that avoids ray double counting," *IEEE Antennas and Propagation Society International Symposium. 2001 Digest*. Boston, MA, USA, 2001, pp. 464-467.

[11] S. Kasdorf, B. Troksa, J. Harmon, C. Key, and B. M. Notaros, "Shooting-Bouncing-Rays Technique to Model Mine Tunnels: Theory and Accuracy Validation," *Proceedings of the 2020 International Applied Computational Electromagnetics Society (ACES) Symposium – ACES2020*, July 27–31, 2020, Online Conference.

[12] C. Key, B. Troksa, F. Kunkel, S. V. Savic, M. M. Ilic, and B. M. Notaros, "Comparison of Three Sampling Methods for Shooting-Bouncing Ray Tracing Using a Simple Waveguide Model,"

Proceedings of the 2018 IEEE International Symposium on Antennas and Propagation, July 8–13, 2018, Boston, MA, USA, pp. 2273–2274.

[13] V. Orlovsky, "Decimal expansion of radius of inscribed sphere about a regular icosahedron with edge = 1," The On-Line Encyclopedia of Integer Sequences. Jul. 2010.

[14] A. C. Yucel, W. Sheng, C. Zhou, Y. Liu, H. Bagci and E. Michielssen, "An FMM-FFT Accelerated SIE Simulator for Analyzing EM Wave Propagation in Mine Environments Loaded With Conductors," in *IEEE Journal on Multiscale and Multiphysics Computational Techniques*, vol. 3, pp. 3-15, 2018.

[15] D. G. Dudley, M. Lienard, S. F. Mahmoud and P. Degauque, "Wireless propagation in tunnels," *IEEE Antennas and Propagation Magazine*, vol. 49, no. 2, pp. 11-26, April 2007.

Stephen Kasdorf Received B.S. (magna cum laude) degrees in 2019 in both electrical engineering and applied physics from Colorado State University. He is currently working towards a PhD in electrical engineering at Colorado State University. His research interests include high frequency asymptotic electromagnetics methods such as ray optics and physical optics, as well as their hybridization with full-wave numerical techniques.

Blake Troksa was born in Boulder, CO in 1996. He received his B.S. (2018) and his M.S. (2019) in Electrical and Computer Engineering from Colorado State University. He is currently working as a software development engineer in the area of cloud computing. His research interests include hardware acceleration and distributed systems.

Cam Key (S'16) was born in Fort Collins, CO in 1996. He received his B.S. (2018) and his Ph.D. (2020) in Electrical and Computer Engineering from Colorado State University. His current research interests include uncertainty quantification, error prediction, and optimization for computational science and engineering; computational geometry, meshing, data science, machine learning, artificial intelligence, remote sensing and GIS, and novel applications of numerical methods across disciplines.

Jake Harmon (S'19) was born in Fort Collins, CO in 1996. He received his B.S. (*summa cum laude*) in 2019 and is currently pursuing his Ph.D. in Electrical Engineering from Colorado State University. His current research interests include adaptive numerical methods, uncertainty quantification, computational geometry, and higher order modeling in the finite element method and surface integral equation method of moments.

Branislav M. Notaroš (M'00-SM'03-F'16) received the Dipl.Ing. (B.S.), M.S., and Ph.D. degrees in electrical engineering from the University of Belgrade, Belgrade, Yugoslavia, in 1988, 1992, and 1995, respectively. From 1996 to 1999, he was Assistant Professor in the School of Electrical Engineering at the University of Belgrade. He was Assistant and Associate Professor from 1999 to 2006 in the Department of Electrical and Computer Engineering at the University of Massachusetts Dartmouth. He is currently Professor of Electrical and Computer Engineering, University Distinguished Teaching Scholar, and Director of Electromagnetics Laboratory at Colorado State University. Dr. Notaroš serves as General Chair of the 2022 IEEE International Symposium on Antennas and Propagation and USNC-URSI National Radio Science Meeting and is Associate Editor for the IEEE Transactions on Antennas and Propagation and member of the IEEE Antennas and Propagation Society Administrative Committee. He serves as President of Applied Computational Electromagnetics Society (ACES) and as Chair of USNC-URSI Commission B. He was the recipient of the 2005 IEEE MTT-S Microwave Prize, 1999 IEE Marconi Premium, 2019 ACES Technical Achievement Award, 2015 ASEE ECE Distinguished Educator Award, 2015 IEEE Undergraduate Teaching Award, and many other research and teaching international and national awards.